

NJC

Accepted Manuscript



This is an *Accepted Manuscript*, which has been through the Royal Society of Chemistry peer review process and has been accepted for publication.

Accepted Manuscripts are published online shortly after acceptance, before technical editing, formatting and proof reading. Using this free service, authors can make their results available to the community, in citable form, before we publish the edited article. We will replace this *Accepted Manuscript* with the edited and formatted *Advance Article* as soon as it is available.

You can find more information about *Accepted Manuscripts* in the [Information for Authors](#).

Please note that technical editing may introduce minor changes to the text and/or graphics, which may alter content. The journal's standard [Terms & Conditions](#) and the [Ethical guidelines](#) still apply. In no event shall the Royal Society of Chemistry be held responsible for any errors or omissions in this *Accepted Manuscript* or any consequences arising from the use of any information it contains.



www.rsc.org/njc

Synthesize cathode material $\text{Li}_3\text{V}_2(\text{PO}_4)_3/\text{C}$ of Li-ion batteries by using PVDF as carbon source

Lingfang Li^{1,2} Changling Fan^{1*} Xiang Zhang¹ Taotao Zeng¹ Weihua Zhang¹ Shaochang Han¹

¹ College of Materials Science and Engineering, Hunan University, Changsha 410082, P.R.China

² College of Mechanical Engineering, Hunan University of Arts and Science, Changde, 415000, P.R.China

* Correspondence to,

Address, College of Materials Science and Engineering, Hunan University, No. 2, South

Lushan Road, Changsha 410082, PR China

Tel., +86 731 88822967; Fax, +86 731 88822967

E-mail address, clfanhd@yahoo.com.cn (C.-L. Fan)

Abstract: By adopting the Polyvinylidene Fluoride (PVDF) as carbon source, here we present the synthesizing of two samples of cathode material $\text{Li}_3\text{V}_2(\text{PO}_4)_3/\text{C}$ via solid state method and a hybrid sol-gel method, which were marked as LVP-1 and LVP-2. The electrochemical testing and XRD, SEM, TEM and EIS results showed their electrochemical performance and micro-morphology. The pyrolitic carbon of the polymer PVDF seems like a folded film and forms a conductive net to enhance the electrochemical performance of $\text{Li}_3\text{V}_2(\text{PO}_4)_3$ efficiently. We can speculate that the pyrolitic carbon of polymer is easier to coat on the $\text{Li}_3\text{V}_2(\text{PO}_4)_3$ particle than that of organic carbon materials. Comparing with the solid-state method, the sol-gel method with the combination of surfactant Cetyl Trimethyl Ammonium Bromide (CTAB) is beneficial to control the particle size of cathode material at nano-level. The sample LVP-2 has fairly outstanding rate and cycle performances, which has capacity higher than 90 mAh/g at 15 C and keeps capacity retention of almost 100% after 50 cycles at 5C in 3.0-4.3V (the theoretical capacity is 130 mAh/g in 3.0-4.3V).

Keywords: $\text{Li}_3\text{V}_2(\text{PO}_4)_3/\text{C}$; PVDF; sol-gel method; solid state method; CTAB

1. Introduction

Lithium-ion batteries have attracted phenomenal interest in the portable electronics market and for the future energy demands owing to its higher energy density, long cycle life, compactness and flexibility in design^[1-3]. In recent decades, $\text{Li}_3\text{V}_2(\text{PO}_4)_3$ (LVP) or some other V-based phosphates, which has comparable high potential plate-form, remarkable electrochemical performance and stable crystalline lattices, is of more and more interest as electrodes in lithium-ion energy storage devices^[4-8]. There are lots of synthesizing methods such as solid state method^[9-13], sol-gel method^[14-16], hydro-thermal method^{[17][18]}, microwave method^{[19][20]}, spray-drying method^{[21][22]}, and so on. Among them the most widely used are the first two. The technology of solid state method is simple but the particle size is hard to control because of the high sintering point. The sol-gel method is conducive to get finer particle because the raw materials are dissolved in solvent and mixed at molecular level. In this study, we present the different influence of these two methods to the performance of $\text{Li}_3\text{V}_2(\text{PO}_4)_3$.

In our and others' previous research, it was found that polymer carbon source was beneficial to enhance the electrochemical of $\text{Li}_3\text{V}_2(\text{PO}_4)_3$, such as phenolic resin^[23], epoxy resin^[24], thiophene^[25] and so on^{[26][27]}. Thus, the influence of Polyvinylidene Fluoride (PVDF) by playing the role of carbon source was researched in this paper, which was not researched systematically in recent references. PVDF is a kind of translucence or white powder (particle) and its molecular chains packed closely. The short chemical bond of C-F and hydrogen ion forms a stable and tight structure. Its network pyrolytic carbon can not only be used as reductant to reduce V^{5+} to V^{3+} , but also enhances the electro-conductivity of cathode material efficiently.

2. Experimental

Samples preparation

The stoichiometric ratio of raw materials is V_2O_5 : $\text{H}_2\text{C}_2\text{O}_4$: Li_2CO_3 : $\text{NH}_4\text{H}_2\text{PO}_4$: CTAB=1:3:1.5:3:0.1 ($\text{H}_2\text{C}_2\text{O}_4$ and CTAB were only used in hybrid sol-gel method). According to the TG-DSC results of PVDF (Fig.1, at heating rate of $5^\circ\text{C}/\text{min}$ in Argon atmosphere), the pyrolytic carbon is 23% by weight of raw material and the curing temperature and carbonization temperature are shown in DSC curves. The carbon was used not only as reducing agent but also as the coating material to enhance the electrical conductivity. The usage of carbon sources was based on the following principle. Except the reducing carbon which reduces V^{4+} to V^{3+} , the

theoretical excess carbon is 5% by weight of the composite. That is to say, $W_c/(W_c+W_{LVP})=5\%$ (W represents weight). The actual residual carbon contents need to be tested by element analysis.

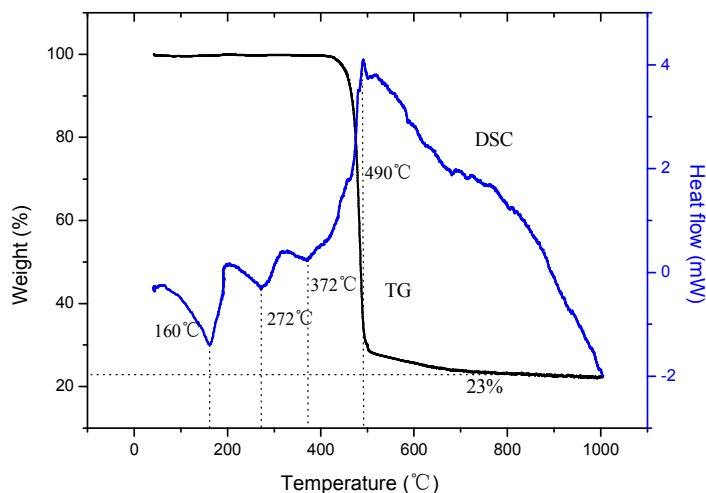


Fig.1 TG-DSC curves of PVDF

The process of conventional solid-state synthesizing is as follows. All the raw materials, V_2O_5 , Li_2CO_3 , $NH_4H_2PO_4$ and PVDF, were dispersed in absolute ethyl alcohol and then thoroughly ground by ball milling for 3 h. The mixture was dried in a vacuum oven for 24 h. Finally, under the atmosphere of Argon, it was heated to 400 °C for 5 h to remove H_2O , NH_3 , HF and CO_2 and then sintered at 800 °C for 16 h to reduce the V^{5+} to V^{3+} . The final sample was marked as LVP-1.

Meanwhile we want to research the influence of PVDF on $Li_3V_2(PO_4)/C$ synthesized by sol-gel method. But the problem is that the solvent of sol-gel method is usually deionized water and polymer materials are water insoluble. For this reason, we combined sol-gel and solid state method together and that's why we called this method the hybrid sol-gel method. The process of it is as follows. First, V_2O_5 and $H_2C_2O_4$ were magnetic stirred in deionized water at 60 °C until the blue VOC_2O_4 solution formed. Second, Li_2CO_3 and $NH_4H_2PO_4$ were added in this solution in turn. Both processes were with gas generating and a hydrophilic homogeneous colloid was formed. Third, the aqueous suspension of Cetyltrimethyl Ammonium Bromide (CTAB) was added as cationic surfactant. Driven by Coulomb force, CTAB captured the anionic LVP colloid, which rearranged the charge density and formed composite micelles in the solution^[28]. Finally,

The final green sol was dried at 80 °C in vacuum oven to obtain gel, then the precursor powder was formed by heating the gel at 400 °C for 5 h under Argon flow. To synthesize the composite material, PVDF and precursor powder were ball-milled together in absolute ethyl alcohol for 2 h and then sintered at 700 °C for 10 h in vacuum tube furnace in Argon.

Preparation of cathode films

The positive electrodes comprised 80-wt.% active materials, 10-wt.% carbon black and 10-wt.% polyvinylidene fluoride (PVDF). These components were mixed in N-methyl-2-pyrrolidone (NMP) and the resulting slurry was coated onto aluminum foil. After the NMP evaporated, electrodes were pressed and punched into a disc with an active area of 1.54 cm² and an active loading of ~5 mg·cm⁻². The precise mass of active material on each positive plate was weighted by an electronic balance with accuracy of 0.0001 g. The electrolyte consisted of 1 M solution of LiPF₆ in a mixture of 1:1 by weight of ethylene carbonate (EC) and dimethyl carbonate (DMC), and lithium metal was chosen as the negative material. The coin-cells (CR2016 size) were fabricated in an argon-filled glove box with a porous polypropylene membrane as the separator.

Sample characterization

The structural analysis of the samples was performed by the XRD using a diffractometer (D/max 2500VB, Japan) in the 2θ range from 10°~70°. The morphology of active materials was observed using (SEM QUANTA 200, USA) and TEM (JEOL-2100F, Japan). TG-DSC analysis was performed by thermal analyser (STA449C, Germany). The content of residual carbon was tested by carbon and sulfur analyzer (EMIA- 8100, Japan). The charge-discharge performance was tested on a multi-channel battery test system (CT2001A, China) in the voltage range of 3.0~4.3 V. The electrochemical impedance spectroscopy (EIS) test was performed on the electrochemical workstation (CHI660C, China) at the frequency range of 10⁵-10⁻² Hz.

3. Results and discussion

Structural characterizations of samples

The X-ray diffraction (XRD) patterns of composite materials which indicate the formation of a high crystalline phases are presented in Fig.2. All the diffraction peaks were indexed to the monoclinic Li₃V₂(PO₄)₃ phase (JCPDS 97-016-1335, space group (P2₁/n)). The diffraction peaks were refined by using software *JADE* and the calculating lattice parameter values are

$a=8.565(8)\text{\AA}$, $b=8.596(7)\text{\AA}$, $c=12.012(7)\text{\AA}$, $\beta=90.491(6)^\circ$ for LVP/1 and $a=8.583(2)\text{\AA}$, $b=8.553(7)\text{\AA}$, $c=11.984(1)\text{\AA}$, $\beta=89.970(6)^\circ$ for LVP/2. These data agree well with the previous literature which proves that the lattice distortion doesn't exist^{[29][30][31]}. Additionally, no peaks attributed to other impurities and crystal carbon were detected from the XRD patterns.

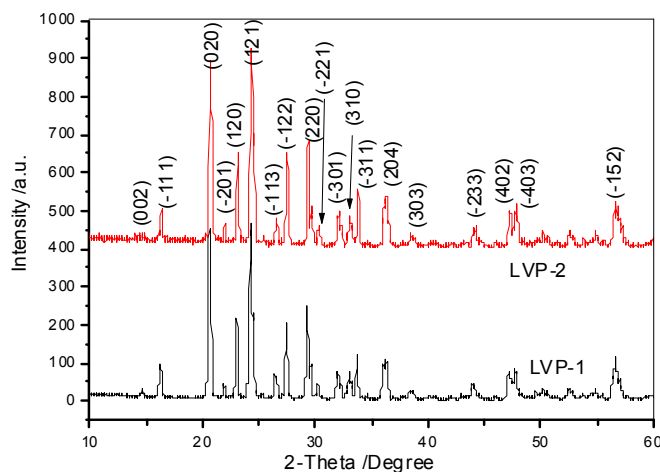


Fig.2 X-ray diffraction patterns of LVP-1 and LVP-2

The scanning electron microscopy (SEM) and transmission electron microscopy (TEM) were used to characterize the detailed structure and morphology of materials. Fig.3 shows the SEM images of two samples. Comparing with LVP-2, the particles of sample LVP-1 are much bigger and the size is nonuniform. The particles of LVP-2 are with an average size of about 0.5 μm , with homogeneous distribution. We believe that the sol-gel method realized the uniform mixing of raw materials in liquid phase and prevent particles from agglomeration. Furthermore, the rejuvenation effect of surfactant CTAB helped the further refinement of particles. However, it worth mentioning that some nanowires with the width of 20-30 nm and length of 1 μm appears in sample LVP-2. This nanowire is another morphology of LVP which is resulted by the self-assembly of organic surfactant and the hydrolysis of LVP colloids, according to the explanation of Wei QL^[31]. Driven by Coulomb force, the added cationic surfactant CTAB captured the anionic LVP colloids, which rearranged the charge density and formed composite micelles in the solution. During the drying process at 80 $^\circ\text{C}$, some organic molecules located in the interstitial space of the aggregated composite assembled into meso-channels. Meanwhile the self-assembly of organic surfactants and the hydrolysis of LVP colloids resulted in the nanowire morphology. Wei^[31] had transferred the solution to a Teflon lined autoclave and kept in an oven

at 180°C for 48 h thus the reaction was completely done and all LVP colloids became nanowires.

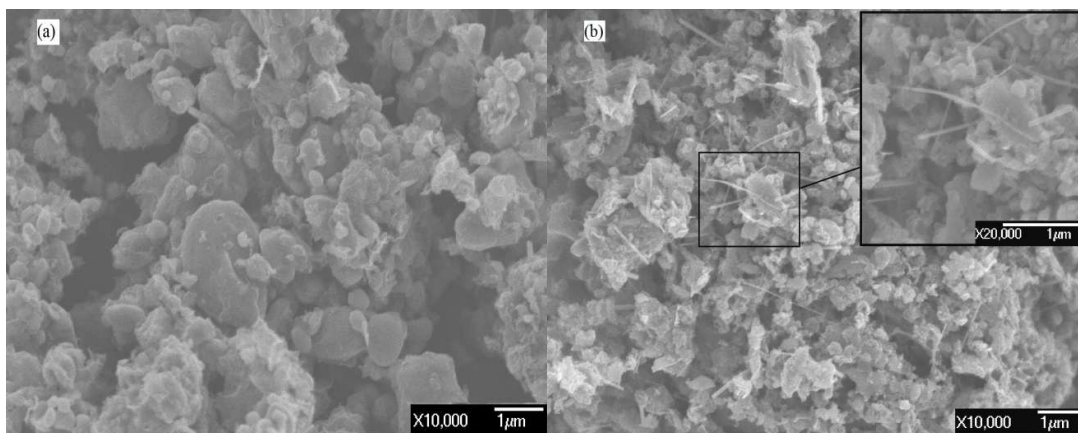


Fig.3 The SEM images of the samples , (a)LVP-1; (b) LVP-2

Fig.4 shows several TEM images of sample LVP-2 which indicate the nanocrystals clearly. Furthermore, we can clearly observe that the morphology of pyrolytic carbon of polymer material is totally different from other carbonaceous materials such as glucose^[32], stearic acid^[33], cyclodextrin^[34] and so on . In Fig.4, the left four are at the same amplification factor. The particles are suborbicular or elliptic and covered by a thin carbon film with fairly large area. Particle II has very uniform and perfect carbon layer all around of it, just like the fruit peel. But not every particle has such a perfect carbon layer and most of them are similar to III or IV, like moon surrounded by some cloud. In spite of this, this kind of chiffon-like carbon layer works like a conductive network to help the electron move faster. The right two express the carbon layer more clearly. The layer may be stripped from the particle surface in the process of ultrasonic dispersion and the thickness of it is about 5-10 nm. The amorphous residual carbon, whose content is 4.91% and 6.72% in LVP-1 and LVP-2 respectively by element analysis, can not only be used as conductive agent to improve the conductivity, but also prevents the direct contact of LVP particles and electrolyte and restrains the dissolution of vanadium ion into electrolyte. And further, it reduces the polarization phenomenon of cathode material significantly.

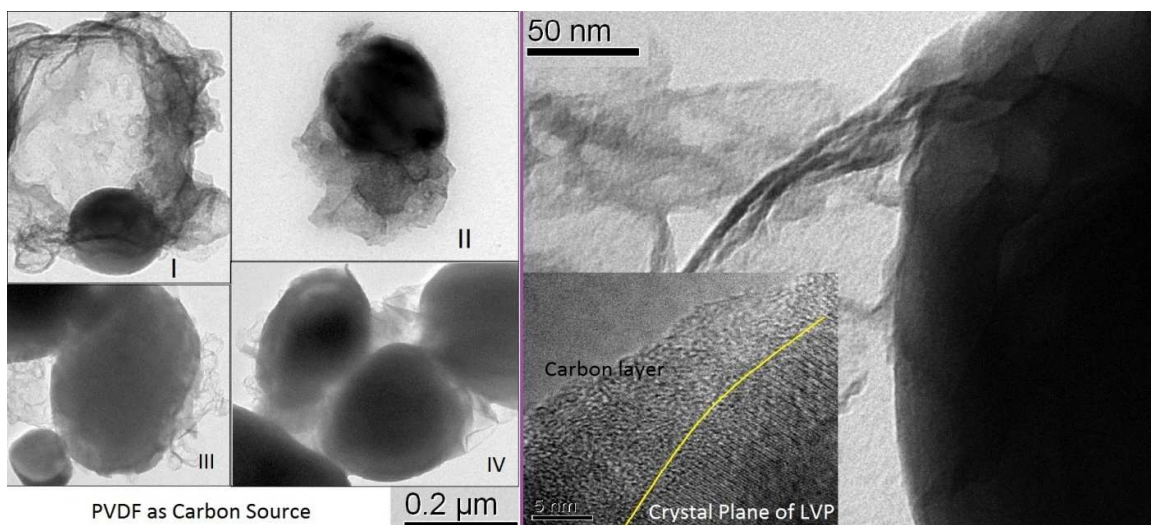


Fig.4 TEM patterns of sample LVP-2

Electrochemical performances

The lithium storage performance was investigated by using CR2016 coin-cells. Curves in Fig.5 describes the charge/discharge performance at different rates. Along with the rate increasing, the capacity dropping of LVP-1 is much faster than LVP-2. When the rate is equal to or less than 2 C, both of them keep the capacity of 120 mAh/g, which is close to the theoretical capacity of 130 mAh/g in 3.0-4.3 V. But capacity of LVP-1 drops to 105 mAh/g at 5 C, 87 mAh/g at 10 C and even 45 mAh/g at 15 C. Meanwhile, capacity of LVP-2 is 115 mAh/g, 103 mAh/g and 96 mAh/g at these three rates respectively. Rate performance of LVP-2 obviously surpasses LVP-1. Dot graphs in Fig.6 shows the cycle performance of two samples by cycled 50 times at 5 C rate uninterruptedly. The small illustration is the charge/discharge curves of two samples at 5 C. At the end of test, the capacity of LVP-1 faded from 102.9 mAh/g to 96.3 mAh/g but capacity of LVP-2 was almost unabated and kept at 110 mAh/g stably. We can conclude that the sample LVP-2, which is synthesized by sol-gel method and used CTAB as surfactant, has better rate performance and more stable cycle performance. This gives $\text{Li}_3\text{V}_2(\text{PO}_4)_3$ a promising commercial future because people have more requests to the charge/discharge speed and life-cycle of Li-ion batteries at this modern society. Fig.7 shows the charge-discharge curves of samples at different rate (0.2 C, 0.5 C, 1 C, 2 C, 5 C, 10 C, 15 C). At the rate less than and equal to 1 C, both exhibit three distinct pairs of charge/discharge plateaus located at around 3.61/3.58 V, 3.69/3.63 V, 4.09/4.03V and the potential difference between charge and discharge at 0.2 C

are fairly low. These prove that these two kinds of samples can maintain stable potential when charging and discharging.

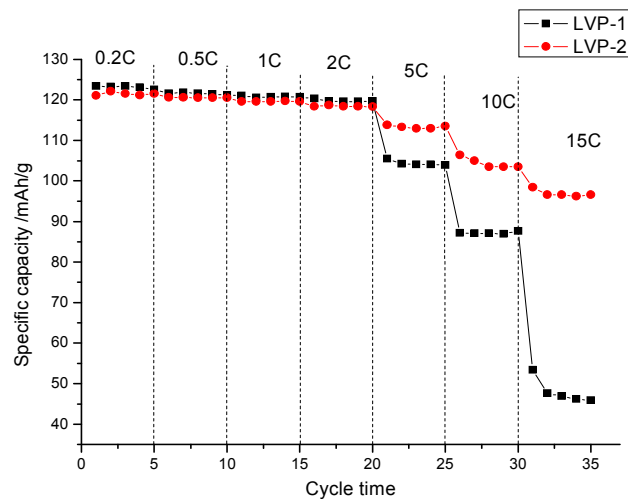


Fig.5 Capacity of samples at different rates

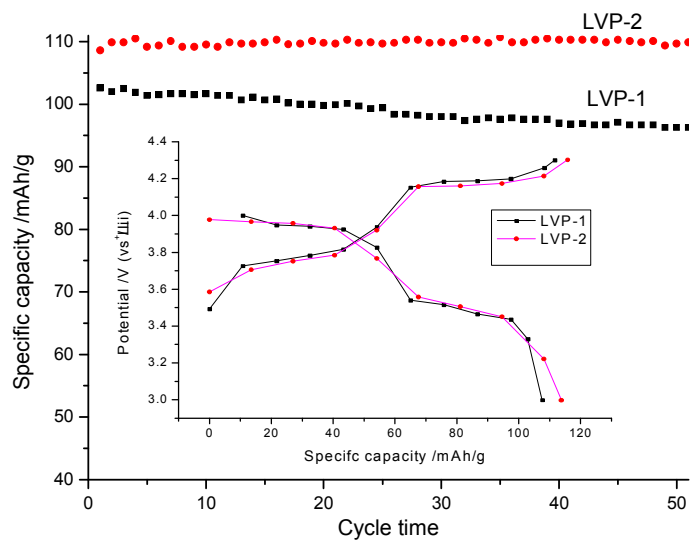


Fig.6 The cycle performance of samples by cycling 50 times under 5C rate

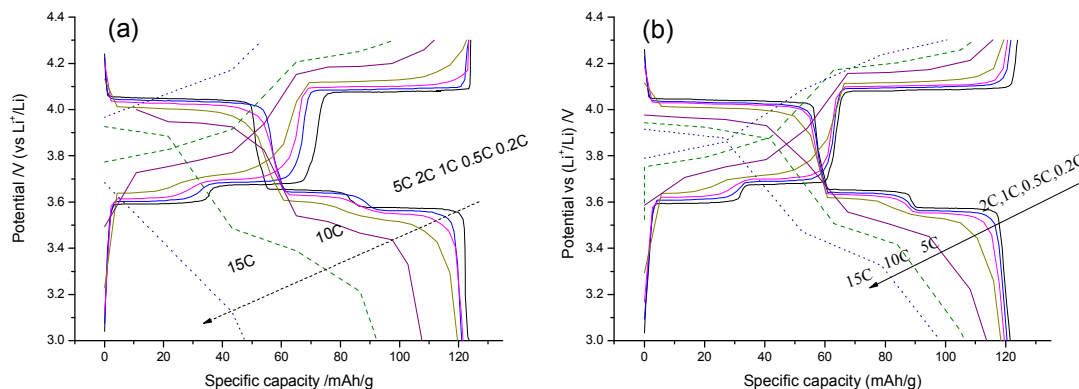


Fig.7 The charge/discharge curves of sample LVP-1 and LVP-2 at various rates

To demonstrate the Li-ion kinetics and structural stability during electrochemical charge/discharge process, a cyclic voltammetry (CV) studies were conducted and presented in Fig.8, with scanning rate of 0.1 mV/s. The mass of active material is 2.2 mg for LVP-1 and 3.6 mg for LVP-2 (These two samples weren't filmed simultaneously and their particle sizes are differ, so the active masses differ quite a bit). According to the principle of cyclic voltammetry, the reversibility of the redox reaction can be confirmed by the overlapping CV curves and similar redox potentials of the subsequent cycles. Furthermore, the electrode reaction rate is limited by the Li^+ diffusion inside the electrode system^[35]. The potential differences between cathodic peak and anodic peak are almost the same to LVP-1 and LVP-2, which is less than 0.15 V. This indicates their nice reversibility at the process of intercalation/deintercalation. The relationship of i_p , scanning rate V and Li^+ diffusion rate D is $i_p = 2.69 \times 10^5 n^{3/2} A D^{1/2} V^{1/2} C$ ^[36], where A is the contact area of electrode with electrolyte (here the geometric area of electrode is used for simplicity, 1.54 cm^2); n is the amount of transferred charges; C is bulk concentration of Li^+ ($3.7 \times 10^{-3} \text{ mol/cm}^3$, calculated from the volume of LVP, 899.8 \AA^3), V is the potential scan rate (here is 0.1 mV/s)^[37]. In short, the relationship between i_p and $V^{1/2}$ is a straight line through the origin and the square of its slope is the diffusion rate D at every peak. It is worth noting that the i_p of LVP-1 is about half of LVP-2, then Li^+ diffusion coefficient of LVP-1 is just quarter of LVP-2, according to the formula (both are in the range of $10^{-8} \sim 10^{-7} \text{ cm}^2/\text{S}$). The Li^+ diffusion coefficient directly decides the charge/discharge

capacity at large rate and that explained why rate performance of LVP-2 is much better than LVP-1.

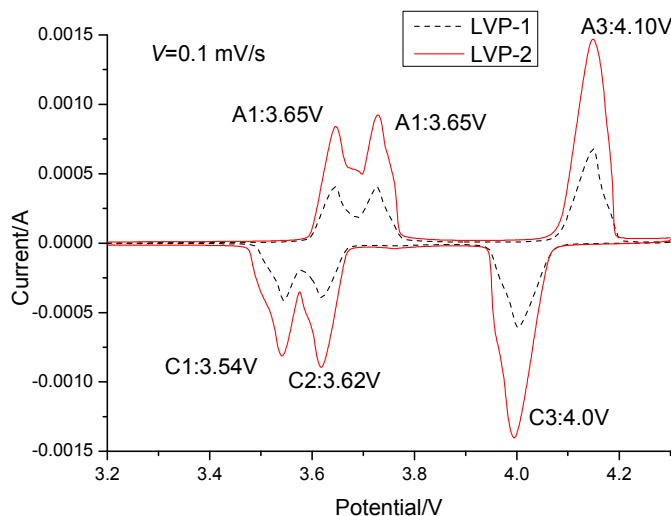


Fig.8 Cyclic voltammogram of two samples

Fig.9 shows the Electrochemical Impedance Spectroscopy (EIS) of samples and the data was fitted by *ZSimpWin* software. The equivalent circuit was inserted in the top left corner of Fig.8a. R_{ct} represents the charge-transfer resistance which reflects the ease or complexity of reaction. The lower value it is, the more beneficial it is to the kinetic process of electrochemical reaction^[38]. R_s represents the electrolytic resistance and it equals to the intersection of the semicircle to X axis. Measurements were carried out at 3.6 V, 3.7 V and 4.1 V potential plateaus in the frequency range of 10^5 - 10^{-2} Hz and it was found that the charge-transfer resistance meets its minimum value at 4.1 V. At this potential, R_{ct} of LVP-1 and LVP-2 is 65.5 Ω and 36.8 Ω respectively and the fresh cell we synthesized previously^[23] has much larger R_{ct} of 184.6 Ω . By comparison, R_{ct} of LVP-2 is not only smaller than LVP-1, but also smaller than the samples synthesized by solid state method with other carbon sources^[39-41]. Furthermore, it is almost close to the advanced study about V-based cathode materials^{[30][42][43]}. The electrolyte resistance was found to be 2.5~3.5 Ω for two samples at different potential. The impedance values clearly show lower charge transfer resistance and electrolytic resistance due to nice electrode kinetics.

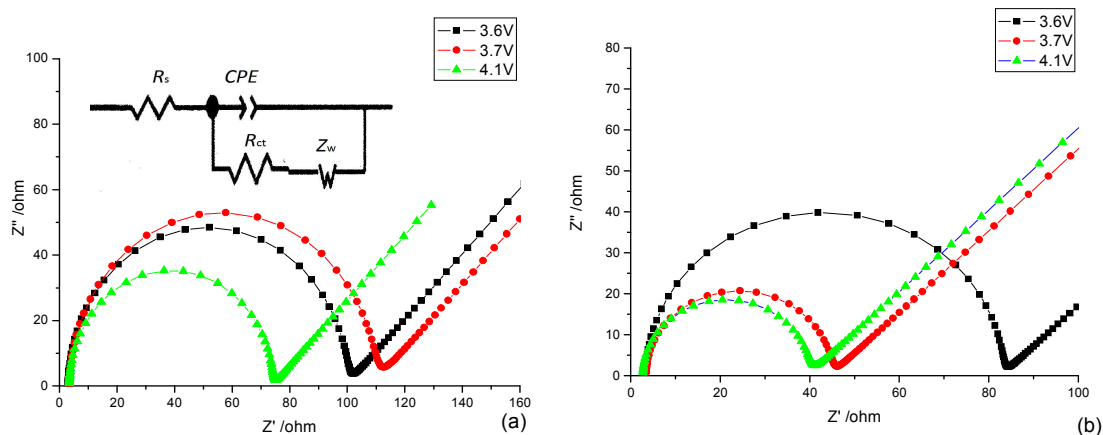


Fig.9 The Nyquist plot of (a) LVP-1; (b) LVP-2 at various potential during charging cycle

4. Conclusion

In summary, we have developed a convenient hybrid sol-gel strategy and adopted Polyvinylidene Fluoride as carbon source and then the composite material $\text{Li}_3\text{V}_2(\text{PO}_4)_3/\text{C}$ was synthesized, by using Cetyltrimethyl Ammonium Bromide as surfactant. Polyvinylidene Fluoride is such a good carbon source whose pyrolytic carbon forms the film-like conductive network to enhance the conductivity of cathode material. Two samples, which are synthesized by solid state method and hybrid sol-gel method, all have stable and high capacity, nice reversibility and high Li^+ diffusion coefficient. Furthermore, the combined action of sol-gel method and surfactant controlled the particle size at the nanometer level and then polarization phenomenon is well controlled and charge transferring resistance is lowered. The uniform carbon-coating and fine particles help LVP-2 to own better rate and cycle performance. It has capacity of 100 mAh/g at 15 C and it cycled 50 times at 5 C rate without any capacity attenuation. Such kind of fairly good charge-discharge capacity and stable cycle performance, gives the $\text{Li}_3\text{V}_2(\text{PO}_4)_3/\text{C}$ synthesized in this method a hopeful application prospect.

Acknowledgments

This work was funded by the National Science Foundation of China (Grant No. 51172068), the Youth Project of Education Department of Hunan province (Grant No. 14B126), the Construct Program of the Key Discipline in Hunan Province (Mechanical Design and Theory) (XJF2011[76]).

References

- [1] M.V. Reddy, G.V. Subba Rao, B.V.R. Chowdari, *Chem. Rev.*, 2013, **113**, 5364
- [2] B.L. Ellis, K. Town, L.F. Nazar, *Electrochim. Acta*, 2012, **84**, 145.
- [3] J.B. Goodenough, Y. Kim, *Chem. Mater.*, 2010, **22**, 587–603
- [4] H. Huang, T. Faulkner, J. Barker, M.Y. Saidi, *J. Power Sources*, 2009, **189**, 748.
- [5] S.C. Yin, H. Grondy, P. Strobel, M. Anne, L. F. Nazar, *J. Am. Chem. Soc.*, 2003, **125**, 10402
- [6] A. Shahul Hameed, M.Nagarathinam, M. Schreyer, *J.Mater. Chem. A*, 2013, **1**, 5721
- [7] A. Shahul Hameed, M.Nagarathinam, M.V. Reddy, *J.Mater. Chem.*, 2012, **22**, 7206
- [8] M.Nagarathinam, K. Savavanan, E.J.H. Phua, *Angew. Chem. Int.*, 2012, **51**, 5866
- [9] M.Y. Saidi, J. Barker, H. Huang, *J. Power Sources*, 2003, **119**, 266.
- [10] H. Huang, S.C. Yin, T. Kerr, *Adv. Mater.*, 2002, **14**, 1525.
- [11] J. Barker, M.Y. Saidi, J.L. Swoyer, *J. Electrochem. Soc.*, 2003, **150**, A684.
- [12] P. Fu, Y.M. Zhao, Y.Z. Dong, *Electrochim. Acta*, 2006, **52**, 1003.
- [13] L.J. Wang, X.C. Zhou, Y.L. Guo. *J. Power Sources*, 2010, **195**, 2844.
- [14] Y.Z. Li, Z. Zhou, X.P. Gao, *Electrochim. Acta*, 2007, **52**, 4922.
- [15] Q. Zhang, Y.H. Li, S.K. Zhong, *Trans. Nonferrous Met. Soc. China*, 2010, **20**, 1545.
- [16] W. Yuan, J. Yan, Z.Y. Tang, *J. Power Sources*, 2013, **17**, 301.
- [17] C. Chang, J. Xiang, X. Shi, *Electrochim. Acta*, 2008, **54**, 623.
- [18] F. Teng, Z.H. Hu, X.H. Ma, *Electrochim. Acta*, 2013, **91**, 43.
- [19] H.P. Liu, S.F. Bi, G.W. Wen, *J. Alloys Compd.*, 2013, **543**, 99.
- [20] J. Yan, W.F. Mao, H. Xie, *Mater. Res. Bull.*, 2012, **47**, 1609.
- [21] L. Wu, S.K. Zhong, J.J. Lu, *Mater. Lett.*, 2014, **115**, 60.
- [22] Y. Jiang, W.W. Xu, D.D. Chen, *Electrochim. Acta*, 2012, **8**, 377.
- [23] L.F. Li, S.H. Han, C.L. Fan, *J. Solid State Electrochem.*, 2014, **18**, 1751.
- [24] S.H. Han, K.H. Zhang, L.F. Li, *J. Hunan Univ, Nat. Sci. Ed.*, 2013, **40**, 70.
- [25] M. Hu, J.P. Wei, L.Y. Xing, *J. Power Sources*, 2013, **222**, 373.
- [26] T. Jiang, W.C. Pan, J. Wang, *Electrochim. Acta*, 2010, **55**, 3864.
- [27] R.V. Hagen, A. Lepcha, X.F. Song, *Nano Energy*, 2013, **2**, 304.
- [28] D.Y. Zhao, Y. Wan, W. Zhou, *Ordered Mesoporous Materials*, 2013, **107**, 2821.
- [29] X.J. Zhu, Y.X. Liu, L.M. Geng L.B. Chen. *J. Power Sources*, 2008, **184**, 578

- [30] A. Shahul Hameed, M.V. Reddy, B.V.R. Chowdari, *Electrochim. Acta*, 2014, **128**, 184.
- [31] Q.L. Wei, Q.Y. An, D.D. Chen, *Nano Letters*, 2014, **14**, 1042.
- [32] J.F. Zhang, C. Shen, B.Zhang, *J. Power Sources*, 2014, **267**, 227.
- [33] Y.Q. Qiao, X.L. Wang, J.Y. Xiang, *Electrochim. Acta*, 2011, **56**, 2269.
- [34] L.J. Wang, H.B. Liu, Z.Y. Tang, *J. Power Sources*, 2012, **204**, 197.
- [35] Y. Gao, Z.Y. Tang, *Electrochim Acta*, 2008, **53**, 5071
- [36] J. R. Dahn, J. Jiang, L.M. Moshurchak, M.D. Fleischauer, *J. Electrochem. Soc.*, 2005, **152** , 1283.
- [37] X.H. Rui, N. Ding, J. Liu, C. Li, C.H. Chen, *Electrochim. Acta*, 2012, **55**, 2384.
- [38] M.M. Ren, Z. Zhou, X.P. Gao, *J. Phys. Chem. C*, 2008, **112**, 5689.
- [39] W. He, X.D. Zhang, X.Y. Du, *Electrochim. Acta*, 2013, **112**, 295.
- [40] Y.Q. Qiao, J.P. Tu, J.Y. Xiang *Electrochim. Acta*, 2011, **56** , 4139.
- [41] J. Wang, S.Q. Zheng, M. Hojamberdiev, *Ceram. Int.*, 2014, **40**, 11251.
- [42] M.V. Reddy, G.V. Subba Rao, B.V.R. Chowdari, *J. Mater. Chem.*, 2011, **21**, 10003.
- [43] M.V. Reddy, B.L.W Wen, K.P. Loh, B.V.R. Chowdari, *ACS Mater. Interfaces*, 2013, **5**, 7777.